

This discussion paper is/has been under review for the journal Biogeosciences (BG).
Please refer to the corresponding final paper in BG if available.

Biophysical constraints on gross primary production by the terrestrial biosphere

H. Wang¹, I. C. Prentice^{1,2,3}, and T. W. Davis²

¹Department of Biological Sciences, Macquarie University, North Ryde, Australia

²AXA Chair Programme in Climate and Biosphere Impacts, Grand Challenges in Ecosystems and the Environment, Department of Life Sciences, Imperial College, Ascot, UK

³Grantham Institute for Climate Change, Imperial College, London, UK

Received: 4 February 2014 – Accepted: 4 February 2014 – Published: 25 February 2014

Correspondence to: H. Wang (han.wang@mq.edu.au)

Published by Copernicus Publications on behalf of the European Geosciences Union.

BGD

11, 3209–3240, 2014

Biophysical
constraints on gross
primary production

H. Wang et al.

Title Page

Abstract

Introduction

Conclusions

References

Tables

Figures

⏪

⏩

◀

▶

Back

Close

Full Screen / Esc

Printer-friendly Version

Interactive Discussion



Abstract

Persistent divergences among the predictions of complex carbon cycle models include differences in the sign as well as the magnitude of the response of global terrestrial primary production to climate change. This and other problems with current models indicate an urgent need to re-assess the principles underlying the environmental controls of primary production. The global patterns of annual and maximum monthly terrestrial gross primary production (GPP) by C_3 plants are explored here using a simple first-principles model based on the light-use efficiency formalism and the Farquhar model for C_3 photosynthesis. The model is driven by incident photosynthetically active radiation (PAR) and remotely sensed green vegetation cover, with additional constraints imposed by low-temperature inhibition and CO_2 limitation. The ratio of leaf-internal to ambient CO_2 concentration in the model responds to growing-season mean temperature, atmospheric dryness (indexed by the cumulative water deficit, ΔE) and elevation, based on optimality theory. The greatest annual GPP is predicted for tropical moist forests, but the maximum (summer) monthly GPP can be as high or higher in boreal or temperate forests. These findings are supported by a new analysis of CO_2 flux measurements. The explanation is simply based on the seasonal and latitudinal distribution of PAR combined with the physiology of photosynthesis. By successively imposing biophysical constraints, it is shown that partial vegetation cover – driven primarily by water shortage – represents the largest constraint on global GPP.

1 Introduction

Differences among model predictions of the terrestrial carbon balance response to changes in climate and atmospheric carbon dioxide concentration ($[CO_2]$) remain stubbornly large (Ciais et al., 2013; Friedlingstein et al., 2006; Sitch et al., 2008). After re-analysing coupled climate-carbon cycle model results from Friedlingstein et al. (2006), Denman et al. (2007) revealed disagreements in the overall magnitude of the modelled

BGD

11, 3209–3240, 2014

Biophysical constraints on gross primary production

H. Wang et al.

Title Page

Abstract

Introduction

Conclusions

References

Tables

Figures



Back

Close

Full Screen / Esc

Printer-friendly Version

Interactive Discussion



(positive) climate-CO₂ feedback and also in the responses of key processes – ocean CO₂ uptake, soil organic matter decomposition, and especially terrestrial net primary production (NPP) – to [CO₂] increase and/or climate change. Modelled positive responses of global NPP to [CO₂] varied by a factor greater than five, while the models disagreed even on the sign of the response of global NPP to climate. The more recent Earth System Models (ESMs) in the Coupled Model Intercomparison Project 5 (CMIP5) archive show no better agreement (Ahlström et al., 2012; Anav et al., 2013; Arora et al., 2013; Friedlingstein et al., 2014; Jones et al., 2013; Todd-Brown et al., 2013). Ciais et al. (2013) summarized the CMIP5 carbon-cycle results (their Fig. 6.21) and highlighted the weak land carbon uptake response to both [CO₂] and climate change shown by two “N-coupled” ESMs (models allowing for interactions between the terrestrial C and N cycles). The CMIP5 models collectively show a high bias in the simulation of recent trends in atmospheric [CO₂] because the modelled uptake of CO₂ by the oceans and/or land is too small, being smallest in the N-coupled models (Hoffman et al., 2014). Several “offline” N-coupled land carbon cycle models have also generated contradictory, and in some cases apparently unrealistic, responses of NPP to climate (Thomas et al., 2013; Zaehle and Dalmonech, 2011). These disappointing outcomes of recent model development suggest to us that the controls of NPP, not least the role of nutrient limitations, are inadequately understood and that this is a major impediment to the development of reliable ESMs.

Perusal of the terrestrial ecology literature confirms that there is indeed no consensus on the controls of either GPP or NPP. Some empirical primary production models have continued to rely on correlations with mean annual temperature and precipitation (Del Grosso et al., 2008), even though the positive geographic relationship of GPP or NPP with temperature is almost certainly indirect rather than causative (Bonan, 1993; Garbulsky et al., 2010). There is a strong correlation between the latitudinal gradients of photosynthetically active radiation (PAR) and mean annual temperature; PAR is the driving force of photosynthesis but also constitutes a nearly constant fraction of solar shortwave radiation, which is the driving force of the latitudinal temperature gradient.

**Biophysical
constraints on gross
primary production**

H. Wang et al.

Title Page

Abstract

Introduction

Conclusions

References

Tables

Figures



Back

Close

Full Screen / Esc

Printer-friendly Version

Interactive Discussion



Biophysical constraints on gross primary production

H. Wang et al.

Title Page

Abstract

Introduction

Conclusions

References

Tables

Figures

⏪

⏩

◀

▶

Back

Close

Full Screen / Esc

Printer-friendly Version

Interactive Discussion

It is therefore very likely that the observed global relationships of GPP and NPP to temperature are caused at least in part by this correlation between temperature and PAR. Based on a model simulation, Churkina and Running (1998) assessed the relative importance of different climatic controls (temperature, water availability, PAR) on terrestrial primary production, indicating different controls or combinations of controls to be dominant in different regions. This analysis implicitly discounts the possibility that all three factors could simultaneously limit photosynthesis, and ignores the ubiquitous experimentally observed stimulation of C_3 photosynthesis by increasing $[CO_2]$. It has long been established that agricultural crop production is proportional to the cumulative PAR absorbed by the crop (Monteith and Moss, 1977a, b); yet Pongratz et al. (2012) and others have modelled crop production without considering PAR. Many models have invoked N and/or P limitations as ancillary controls on primary production; Huston and Wolverton (2009) went further, arguing that soil nutrients (rather than climate) *primarily* determine the global pattern of NPP. Finally, Fatichi et al. (2013) claimed that NPP is not controlled by photosynthesis at all, but rather by environmental constraints on growth.

Different explanations of the controls of terrestrial primary production are thus rife in the ecological literature. Yet the choice of model assumptions can imply radically different responses to global change (Wang et al., 2012). It is therefore time for a fundamental re-assessment of the controls of primary production. With this goal in mind, we define a conceptually very simple model for GPP, with no tuneable parameters. The model allows us to explore the consequences (and potentially, the limitations) of the hypothesis that *the primary controls on terrestrial GPP are incident PAR, green vegetation cover and $[CO_2]$* . We consider first a counterfactual, continuously vegetated world in which C_3 photosynthesis operates at its full biophysical potential everywhere, and PAR is not attenuated by atmospheric absorption and clouds. Then we add constraints one by one. The model has the form of a “light use efficiency” (LUE) model (i.e. modelled GPP is proportional to absorbed PAR). However, unlike empirical LUE models, the value of LUE and its variation with environmental factors are derived from first

Biophysical constraints on gross primary production

H. Wang et al.

Title Page

Abstract

Introduction

Conclusions

References

Tables

Figures



Back

Close

Full Screen / Esc

Printer-friendly Version

Interactive Discussion



principles, beginning with the standard model of C_3 photosynthesis (Farquhar et al., 1980). The derivation rests on the “co-limitation” or “co-ordination” hypothesis, which predicts that the photosynthetic capacity of leaves at any location and canopy level acclimates to the prevailing daytime PAR so as to be neither in excess (which would entail additional, non-productive maintenance respiration) nor less than is required for full exploitation of the available PAR. This hypothesis implies that average daily photosynthesis under field conditions is close to the point where the Rubisco- and electron transport-limited rates are equal. The co-limitation hypothesis has strong experimental support, as was recently demonstrated by Maire et al. (2012).

The LUE concept has been applied in diagnostic primary production models, including the Simple Diagnostic Biosphere Model, SDBM (Knorr and Heimann, 1995), the Carnegie–Ames–Stanford Approach model, CASA (Field et al., 1995; Potter et al., 1993), the Simple Diagnostic Photosynthesis and Respiration Model, SDPRM (Badawy et al., 2013), and the widely used algorithms to estimate GPP and NPP from remotely-sensed “greenness” data provided by MODIS (Running et al., 2004). (By diagnostic, we mean models that rely on remotely sensed green vegetation as an input – distinct from prognostic models that simulate vegetation cover.) A particular version of the co-limitation hypothesis was used to derive an explicit LUE formula in the strand of complex, prognostic terrestrial carbon cycle models that originated with BIOME3 (Haxeltine and Prentice, 1996) and the Lund-Potsdam-Jena (LPJ) DGVM (Sitch et al., 2003). CO_2 limitation can be represented in a natural way in the co-limitation framework, if the ratio of leaf-internal to ambient $[CO_2]$ (c_i/c_a) can be specified. This is done here with the help of the “least-cost hypothesis” (Wright et al., 2003), which states that the long-term effective value of c_i/c_a minimizes the combined unit costs of carboxylation (proportional to photosynthetic capacity) and transpiration (proportional to sapflow capacity). This hypothesis also has strong empirical support (Prentice et al., 2013) and provides a continuous prediction of the c_i/c_a ratio as a function of environmental aridity, temperature and elevation. Our modelling approach thus does *not* require that we divide plants into functional types with apparently differing physiological responses, as has

usually been done in complex models, and is now commonly done in models based on remote sensing as well.

We focus exclusively on GPP. It is probably reasonable to extrapolate the first-order results to NPP, given that on a global scale NPP is approximately a constant fraction of GPP (Waring et al., 1998) – although caution is needed because this fraction may vary (DeLUCIA et al., 2007). The fine-tuning of the NPP/GPP ratio is a separate issue, which will be considered in forthcoming work. C_4 and CAM photosynthesis are not modelled. For this reason, evaluation of the model results is based on data from forests, where C_3 photosynthesis predominates.

2 Methods

2.1 Model summary and protocol

The model was applied to the global land surface, excluding ice-covered regions and Antarctica, at a grid resolution of 0.5° . It was driven with a fixed seasonal cycle of PAR and climate. Insolation (shortwave solar radiation at the top of the atmosphere) was computed using standard methods. Half of solar shortwave radiation was assumed to be PAR. PAR was converted from energy to photon units using a conversion factor of 4.5 MJ mol^{-1} . Remotely sensed green vegetation cover data were used to derive absorbed PAR. Required climate data (mean monthly temperature, precipitation and fractional cloud cover) were derived from Climate Research Unit data (CRU TS3.1), averaged over the same period as the remote sensing measurements.

We first considered a hypothetical world in which PAR at the top of the atmosphere (PAR_{toa} , see more detailed calculations in Sect. A1) could be fully utilized by plants. In other words, we assumed a continuous vegetation cover, ideal temperature and moisture conditions, and a perfectly clear atmosphere containing adequate CO_2 for optimal photosynthesis (Table 1). Potential GPP under these conditions is the product of PAR_{toa} , leaf absorptance (a), and the intrinsic quantum efficiency of photosynthesis

BGD

11, 3209–3240, 2014

Biophysical constraints on gross primary production

H. Wang et al.

Title Page

Abstract

Introduction

Conclusions

References

Tables

Figures

⏪

⏩

◀

▶

Back

Close

Full Screen / Esc

Printer-friendly Version

Interactive Discussion



(φ_0). The leaf absorptance accounts for the fraction of PAR lost by reflection (albedo), transmission, and incomplete utilization of the PAR spectrum. We assumed a leaf absorptance of 0.8 (Collatz et al., 1998) – bearing in mind that this quantity shows substantial variation among species (Long et al., 1993). The intrinsic quantum efficiency of photosynthesis is the LUE (mol mol^{-1}) that can be realized at low PAR, low $[\text{O}_2]$ and saturating $[\text{CO}_2]$. We assigned an intrinsic quantum efficiency of 0.85, again following Collatz et al. (1998). This is in the mid-range of reported values for the intrinsic quantum efficiency of C_3 photosynthesis.

As the real atmosphere is not perfectly clear and contains clouds, we considered next the effect of atmospheric absorption and reflection of PAR. PAR_{toa} for each month of the year was converted to the PAR incident on vegetation canopies (Table 1) using the Prescott formula (Linacre, 1968). This modifies GPP by a factor of 0.75 (the clear-sky transmittivity) under clear skies, declining to 0.25 under completely cloudy skies. The values thus obtained were increased by 2.7 % per km of elevation (Allen, 2005) to account for the reduced thickness of the atmosphere at higher elevations (Eq. A3).

The fraction of absorbed PAR (fAPAR), indicating actual green vegetation cover, was introduced next. fAPAR is assumed to represent effects of limited water availability, low temperatures and nutrient deficits in reducing the NPP available for allocation to leaves as well as the varying phenology and turnover time of leaves (Table 1). It was further assumed that fAPAR implicitly accounts for the differential penetration of diffuse and direct PAR into dense vegetation canopies (Mercado et al., 2009). We used the SeaWiFS fAPAR product (1998 to 2004) (Gobron et al., 2006), which we have previously used to drive the SDBM in a benchmarking study (Kelley et al., 2013). For the present application we averaged different years' values for each month of the year, to produce a monthly climatology of fAPAR. Missing values in winter were set to zero. The monthly values of fAPAR were used to multiply the monthly values of PAR.

In the next step the inhibition of CO_2 assimilation at low temperatures was described by a ramp function, reducing the utilization of PAR for photosynthesis linearly from 10°C to 0°C with zero photosynthesis at daily temperatures below 0°C . Daily values of PAR

BGD

11, 3209–3240, 2014

Biophysical constraints on gross primary production

H. Wang et al.

Title Page

Abstract

Introduction

Conclusions

References

Tables

Figures

⏪

⏩

◀

▶

Back

Close

Full Screen / Esc

Printer-friendly Version

Interactive Discussion



were thus integrated over the month to give monthly PAR_0 , as defined in Table 1. PAR_0 is a weighted monthly PAR, with the weighting provided by the ramp function (Eqs. A4 and A5).

The final step accounts for the effect of photorespiration and substrate limitation at subsaturating $[CO_2]$, based on the Farquhar model (Table 1). GPP was reduced by the factor $(c_i - \Gamma^*) / (c_i + 2\Gamma^*)$ where Γ^* is the photorespiratory compensation point. (The co-limitation hypothesis simply equates the Rubisco- and electron-transport limited rates of photosynthesis. We use the electron-transport limited rate as this yields an estimate of LUE. We neglect J_{max} limitation, thus making the approximation that Rubisco is always limiting at high PAR.) The temperature dependence of Γ^* was described by an Arrhenius function (Bernacchi et al., 2003), evaluated at the growing-season mean temperature ($mGDD_0$). $mGDD_0$ is defined as the annual sum of temperatures above $0^\circ C$ (growing degree days) divided by the length of the period with temperatures above $0^\circ C$. The ratio c_i/c_a was predicted as a function of $mGDD_0$, atmospheric aridity (ΔE) and elevation, based on the least-cost hypothesis (Prentice et al., 2013). ΔE is the cumulative annual difference between actual and equilibrium evapotranspiration, where actual evapotranspiration is computed using a quasi-daily soil-moisture accounting scheme (Cramer and Prentice, 1988). This measure is a proxy for the effective average value of vapour pressure deficit experienced by the plants (Prentice et al., 2013). Further details on the calculation of c_i/c_a are given in Sect. A4.

2.2 Driving data

PAR, PAR_0 , $mGDD_0$ and ΔE were calculated from insolation and climate data with a modified version of the STASH model (Gallego-Sala et al., 2010; Sykes et al., 1996). STASH was modified to account for the effects of elevation on atmospheric transmissivity and the effect of atmospheric pressure on the psychrometer constant, used in the calculation of equilibrium evapotranspiration (<http://www.fao.org/docrep/X0490E/x0490e07.htm>). The algorithm to compute insolation was also revised to more accurately compute celestial longitude (the angle between the Earth's position and its

BGD

11, 3209–3240, 2014

Biophysical constraints on gross primary production

H. Wang et al.

Title Page

Abstract

Introduction

Conclusions

References

Tables

Figures

◀

▶

◀

▶

Back

Close

Full Screen / Esc

Printer-friendly Version

Interactive Discussion



position at the vernal equinox) on each day of the year, given the orbital parameters (eccentricity, obliquity and precession). The method of Kutzbach and Gallimore (1988) was used to represent the effect of precession. (This modification has negligible effect under the present-day orbital configuration.) Elevations were taken to be the mean elevations of each grid cell as given by CRU (http://www.cru.uea.ac.uk/~timm/grid/CRU_TS_2_1.html). [CO₂] was set at its mean value during 1998 to 2005 (370 ppm).

2.3 GPP data-model comparisons

GPP predictions from the final modelling step were compared to the Luyssaert et al. (2007) global synthesis of annual GPP measurements from forests. The model's prediction of global GPP was compared with the range of published, observationally based estimates (Beer et al., 2010).

Modelled seasonal cycles of GPP were compared with seasonal cycles of gap-filled GPP derived from eddy covariance measurements of CO₂ exchange in the FLUXNET archive (<http://www.fluxdata.org/>). One hundred and forty-six flux towers in FLUXNET have publicly available data between 2002 and 2006. We used all of these data. Half-hourly measurement pairs of net ecosystem exchange (NEE) and photosynthetic photon flux density (PPFD) (equivalent to PAR, in photon units) were partitioned into GPP and ecosystem respiration by fitting the rectangular hyperbola response model as presented by Ruimy et al. (1995) (their Eq. 27). Non-linear least-squares regression was performed on each monthly set of NEE-PPFD observation pairs at each tower, after anomalous data points (identified using Peirce's criterion) had been deleted. Monthly totals of GPP were then calculated as follows. First, each PPFD time series was completed using a gap-filling product based on a half-hourly calculation of solar radiation at the top of the atmosphere, scaled down in magnitude by daily observations of short-wave downwelling solar radiation as provided by the WATCH Forcing Data based on the ERA Interim re-analysis (Weedon et al., 2012). Then the gap-filled PPFD data were converted to GPP using the model-fitted parameters for each month and tower,

BGD

11, 3209–3240, 2014

Biophysical constraints on gross primary production

H. Wang et al.

Title Page

Abstract

Introduction

Conclusions

References

Tables

Figures

◀

▶

◀

▶

Back

Close

Full Screen / Esc

Printer-friendly Version

Interactive Discussion



and cumulated to monthly totals. Months for which the data could not be fitted with a rectangular hyperbola were excluded from analysis.

3 Results

3.1 Model predictions: annual GPP

5 The patterns and total values of global annual GPP show a progressive reduction during the course of imposing biophysical and ecophysiological constraints (Fig. 1; Table 1). Potential GPP based on PAR_{toa} varies only with latitude, being maximal at the equator and declining smoothly towards the poles (Fig. 1a). The decline is almost but not quite symmetrical. The Southern Hemisphere shows slightly higher values at any given latitude because the Earth is currently nearest to the Sun in northern winter (southern summer).

10 The strict latitudinal pattern of potential GPP is altered by cloud cover (Fig. 1b). Values are lowered around the equator and at high latitudes due to cloudiness. The highest values are found in subtropical deserts. The combined effects of atmospheric absorption and clouds reduce total global annual GPP by nearly half (Table 1).

15 The largest drop in modelled GPP, by about 78 %, occurs at the next step (Fig. 1c) due to the introduction of fAPAR. Obvious modifications include the effects of low water availability in desert regions. fAPAR values of unity are restricted to a very few locations (e.g. subantarctic islands). Forested regions typically have fAPAR values in the range 20 0.2 to 0.8.

25 Additional effects of temperature limitation, introduced after the influence of fAPAR has been taken into account, further diminish GPP only in those regions of the world (temperate, boreal, polar and high-mountain regions) that routinely experience cold conditions. The reduction in global total annual GPP (Table 1) at this step is only about 7 %.

Biophysical constraints on gross primary production

H. Wang et al.

Title Page

Abstract

Introduction

Conclusions

References

Tables

Figures



Back

Close

Full Screen / Esc

Printer-friendly Version

Interactive Discussion



The effects of subsaturating $[\text{CO}_2]$ in limiting GPP are also relatively slight (30%), but pervasive across terrestrial ecosystems. The strongest CO_2 constraint on GPP is predicted for hot and dry regions such as the Australian deserts; the weakest constraint is predicted for cold and humid regions, such as eastern Siberia.

Elevation effects are slight in a global perspective, although significant locally. A sensitivity test showed that increasing the elevation of the global land surface by 4000 m, with all other factors unchanged, would increase global GPP by 7%. The net effect is positive because the thinner atmosphere (greater PAR transmission) and reduced oxygen partial pressure (greater affinity of Rubisco for CO_2) at high elevations more than counteract the negative effects of the reduced psychrometer constant (increased water loss) and reduced partial pressure of CO_2 .

3.2 Data-model comparisons: annual GPP

The comparison with the Luysaert et al. observations on annual GPP indicates a satisfying model prediction at the high end for tropical forests, but a general tendency to overestimate GPP in temperate and boreal forests (Fig. 2). The predicted global total GPP value (210 PgCa^{-1}) lies above the range of $123 \pm 8 \text{ PgCa}^{-1}$ provided by Beer et al. (2010) based on eddy covariance flux data and various diagnostic models, and also above the larger estimate by Welp et al. (2011), $150\text{--}175 \text{ PgCa}^{-1}$, inferred from oxygen isotope data. Nevertheless, inspection of Fig. 2 suggests that the model approximates a “boundary line” for temperate and boreal forest GPP. A few sites show GPP close to that modelled, but many others show GPP lower than this.

3.3 The seasonal maximum of GPP

Although the greatest annual GPP is both predicted and observed for tropical moist forests (Figs. 1 and 2), the GPP achieved during the month with maximum GPP can be as high or higher in boreal or temperate forests. This tendency is shown both by model predictions (Fig. 3) and flux observations (Fig. 4). Tropical evergreen broadleaf

BGD

11, 3209–3240, 2014

Biophysical constraints on gross primary production

H. Wang et al.

Title Page

Abstract

Introduction

Conclusions

References

Tables

Figures

◀

▶

◀

▶

Back

Close

Full Screen / Esc

Printer-friendly Version

Interactive Discussion



5 forests have high GPP throughout the year, with a muted seasonal cycle reflecting the alternation of wetter and drier seasons (Fig. 4). The estimated average annual GPP of $2760 \text{ gCm}^{-2} \text{ a}^{-1}$ marks tropical forests as the most productive, but the maximum monthly GPP in tropical evergreen broadleaf forests (about $300 \text{ gCm}^{-2} \text{ month}^{-1}$) is exceeded by forests in the temperate zone (Fig. 4). The highest mean monthly GPP values in our flux data set are $358 \text{ gCm}^{-2} \text{ month}^{-1}$ in a temperate evergreen needleleaf forest and $484 \text{ gCm}^{-2} \text{ month}^{-1}$ in a temperate deciduous broadleaf forest. The monthly maximum GPP in boreal forests (in June or July), the lower quartile for temperate deciduous broadleaf forest, and the upper quartile for temperate evergreen and mixed
10 forests are similar to or even larger than the maximum for tropical evergreen broadleaf forests.

Figure 3 provides a biophysically based prediction of this phenomenon. In the top panel, it is already clear that the maximum monthly potential GPP – being proportional to insolation – is greatest in high latitudes, declining towards the equator. This
15 is because the day length in high-latitude summer more than compensates for the low sun angles. The maximum daily insolation at any place and time on the Earth's surface occurs near the polar circles in the days around the summer solstice. High cloud cover (Fig. 3b), low vegetation cover (Fig. 3c) and low temperatures (Fig. 3d) all tend to reduce the maximum monthly GPP in the Arctic, but the basic pattern persists
20 (Fig. 3e) even after all constraints are included, allowing high maximum monthly GPP – comparable to or higher than that in tropical forests – to be achieved in boreal or temperate forests. The highest values of maximum monthly GPP ($> 600 \text{ gCm}^{-2} \text{ a}^{-1}$) are predicted for certain mid-latitude temperate and boreal forest regions, including the Caucasus and Altai mountains.

BGD

11, 3209–3240, 2014

Biophysical constraints on gross primary production

H. Wang et al.

Title Page

Abstract

Introduction

Conclusions

References

Tables

Figures



Back

Close

Full Screen / Esc

Printer-friendly Version

Interactive Discussion



4 Discussion

4.1 Key patterns explained

Our simple model predicts, among other things, that GPP in the summer months can be as high as or higher in boreal or temperate forests than it is in tropical forests. This prediction is supported by flux data (Fig. 4) and consistent with analyses of NPP data by Kerkhoff et al. (2005) and Huston and Wolverton (2009). Huston and Wolverton (2009) attributed this pattern to the prevalence of highly weathered, nutrient-poor soils in the tropics. Our explanation is simpler, based on the latitudinal and seasonal distribution of insolation and cloud cover combined with the physiology of photosynthesis. Although it is likely that variations in soil nutrient status are reflected to some extent in fAPAR (with allocation to leaves being reduced and allocation to fine roots increased under low-nutrient conditions: Poorter et al., 2012), the fact that temperate forests do not consistently have lower fAPAR than tropical forests suggests that this effect is not predominant.

We argue therefore that the first-order latitudinal patterns of GPP and its seasonal cycle are ultimately determined astronomically, by the distribution of insolation. Due to the obliquity of the Earth's axis relative to the ecliptic, the latitude where the Sun is directly overhead swings between the Tropics of Cancer and Capricorn, crossing the equator twice a year. The tropics therefore receive maximum annual insolation. But the maximum insolation in any one month shows a very different pattern, with highest values at high latitudes. At latitudes $> 50^\circ$ in both hemispheres the high maximum monthly insolation is counteracted in its effect on GPP by high cloud cover and seasonally low temperatures. High incident and absorbed PAR are experienced widely in summer in boreal and temperate latitudes, resulting in a high seasonal GPP.

Neither our predictions nor our empirical analysis support Huston and Wolverton's (2009) additional contention that *annual* primary production is as high in temperate and boreal forests as in tropical forests. This is in any case poorly supported by the data they present. Our model is consistent with the general understanding that primary

BGD

11, 3209–3240, 2014

Biophysical constraints on gross primary production

H. Wang et al.

Title Page

Abstract

Introduction

Conclusions

References

Tables

Figures

◀

▶

◀

▶

Back

Close

Full Screen / Esc

Printer-friendly Version

Interactive Discussion



production is highest in tropical forests, due to relatively high insolation and adequate temperature and moisture conditions persisting through the year.

One limitation of our analysis is that we have implicitly assumed that fAPAR is independent of $[\text{CO}_2]$. Thus, the effect of the final constraint – where the effect of sub-saturating CO_2 and with it, the effect of restrictions on c_i and GPP due to stomatal closure in dry environments, are added – reflects only the effects of $[\text{CO}_2]$ on the rate of photosynthesis that could be achieved on the assumption of unchanging vegetation cover. The resulting prediction is a relatively modest potential for increased GPP with increasing $[\text{CO}_2]$, following the $A-c_i$ curve for electron transport-limited photosynthesis. A sensitivity analysis in which $[\text{CO}_2]$ was elevated by 200 ppm yielded a 5 % to 25 % stimulation of modelled annual GPP: smaller than the effect reported for temperate forest NPP ($23 \pm 2 \%$) by Norby et al. (2005) based on Free-Air Carbon dioxide Enrichment (FACE) experiments. This analysis also suggested a strong relationship between CO_2 fertilization and temperature with warm areas experiencing stronger CO_2 fertilization. Annual GPP was predicted to increase by about 18 % across the tropics but by no more than 12 % in the high latitudes of both hemispheres. The relationship to temperature is less marked than in the analysis by Hickler et al. (2008), however. This is because the LPJ-GUESS model as used by Hickler et al. (2008) did not account for the response of c_i/c_a to temperature. In our model, lower c_i/c_a at lower temperatures implies a strengthening of the response to c_a because of the convexity of the $A-c_i$ curve. This strengthening partially counteracts the temperature effect on Γ^* , which tends to produce a stronger CO_2 response at higher temperatures.

Additional effects, not considered here, could modify these model predictions. One is the possible restriction of $[\text{CO}_2]$ fertilization due to exacerbated nutrient shortages, invoked by many authors (e.g. Ciais et al., 2013), which would reduce the potential for GPP to be influenced by $[\text{CO}_2]$. Another is the possible increase of fAPAR resulting from “water saving” by reduced stomatal conductance. Evidence has recently been presented for an increase of fAPAR, independently of precipitation trends, in warm and dry regions (Donohue et al., 2013). Such an increase would also tend to counteract

BGD

11, 3209–3240, 2014

Biophysical constraints on gross primary production

H. Wang et al.

Title Page

Abstract

Introduction

Conclusions

References

Tables

Figures

⏪

⏩

◀

▶

Back

Close

Full Screen / Esc

Printer-friendly Version

Interactive Discussion



any possible increase in runoff due to increasing [CO₂] (Ukkola and Prentice, 2013; Wang et al., 2012).

A novel feature of the model is its inclusion of elevation effects on GPP. Elevation affects GPP in several ways. Enhanced PAR is a direct result of a reduced path length through the atmosphere. Reduced stomatal conductance and c_i/c_a ratios (and correspondingly higher photosynthetic capacity) are predictions of the least-cost hypothesis. These predictions have long-standing empirical support (Friend et al., 1989; Körner and Diemer, 1994), but are accounted for here as a consequence of the reduced partial pressure of O₂, which lowers the cost of carboxylation relative to transpiration. On the other hand, the reduced psychrometer constant tends to increase ΔE . The net effect in our model, *ceteris paribus*, is that GPP increases with elevation. The global effect is small, but the prediction would be worth exploring in the context of elevational transects. It has implications especially for primary production in high-mountain regions in the tropics and subtropics.

The model overestimates GPP in some (not all) temperate and boreal forests. The nature of the scatter in Fig. 2 suggests that the model is predicting an upper bound for GPP, which is not always achieved in the field. There is no systematic difference between broadleaf and needleleaf forests in the extent to which the model overpredicts GPP (Fig. 2). It might be tempting to attribute the variation of observed GPP (corresponding to any one band of predicted GPP) to nutrient limitations, but such a conclusion would be premature, especially as this variation does not seem to apply in tropical forests. Further analysis might explicitly take soil properties into account.

4.2 Implications for modelling strategy

In diagnostic models such as the one presented here, green vegetation cover is directly provided from satellite observations. This tactic sidesteps one of the most serious limitations of current dynamic global vegetation models (DGVMs), namely their (in)ability to realistically predict spatial and temporal patterns of green vegetation cover (Kelley et al., 2013). Despite persistent differences among different satellite-derived

BGD

11, 3209–3240, 2014

Biophysical constraints on gross primary production

H. Wang et al.

Title Page

Abstract

Introduction

Conclusions

References

Tables

Figures

◀

▶

◀

▶

Back

Close

Full Screen / Esc

Printer-friendly Version

Interactive Discussion



Biophysical constraints on gross primary production

H. Wang et al.

Title Page

Abstract

Introduction

Conclusions

References

Tables

Figures

◀

▶

◀

▶

Back

Close

Full Screen / Esc

Printer-friendly Version

Interactive Discussion



fAPAR products (McCallum et al., 2010), the physical definition of fAPAR is clear, and remotely sensed fAPAR values could be evaluated and ultimately improved by systematic comparison with in situ measurements (Pickett-Heaps et al., 2014). By using empirical values of fAPAR, we have been able to focus on other aspects of the control of GPP, without confounding by problems with model-derived estimates of fAPAR.

On the other hand, reliable projection of the effects of future [CO₂] and climate changes demands that fAPAR also be predicted from first principles. There must be a feedback from NPP to fAPAR, because sufficient NPP is required to sustain a given leaf area. Current DGVMs model this feedback implicitly but there has been little effort to evaluate their predictions of fAPAR and its response to environmental changes. When tested, models have been found wanting (e.g. Kelley et al., 2013; Bondeau et al., 1999). The joint prediction of NPP and fAPAR is an important goal for further research.

Appendix A

Estimations on the biophysical constraints in the model

A1 PAR at the top of the atmosphere

Instantaneous solar radiation (insolation) on a horizontal surface at the top of the atmosphere is given by:

$$Q = Q_{sc} d_r (\sin l \cdot \sin \delta + \cos l \cdot \cos \delta \cdot \cos h) \quad (\text{A1})$$

Here, Q_{sc} is the solar constant (1369 W m^{-2}) (Willson and Mordvinov, 2003), d_r is the inverse square of the relative Sun–Earth distance (dimensionless), l is latitude in radians, δ is solar declination in radians, and h is the “hour angle” (the time before or after solar noon, in radians). We use formulae based on the day number to obtain d_r and δ . We assume that over the course of one day there is no variation in d_r or δ . As Q_{sc}

and l do not vary either, we can obtain daily insolation by integrating with respect to h between the hours of sunrise and sunset. The result is:

$$Q = (86400/\pi)Q_{sc}d_r(h_s \cdot \sin l \cdot \sin \delta + \cos l \cdot \cos \delta \cdot \sin h_s) \quad (\text{A2})$$

where h_s is the hour angle of sunset in the unit of radians, given by $h_s = \arccos[-\tan l / \tan \delta]$. 86 400 is the number of seconds in a day. The term in the square brackets has to be set to 1 if it exceeds 1, or -1 if it becomes less than -1 , which are the special cases of polar day and night.

Daily total PAR at the top of the atmosphere is taken to be $0.5 Q$ (in energy units), which is then converted to quantum units (photosynthetic photon flux density) using the factor 4.5 MJ mol^{-1} (a spectrally averaged value for the energy content of 1 mol of photosynthetically active photons). Photon units are preferred because photosynthesis depends on the absorption of a given number of quanta, rather than a given amount of electromagnetic energy. LUE is thus a dimensionless quantity.

A2 Atmospheric transmissivity and cloud cover

Daily solar shortwave radiation (R_{swl}) is given by a modification of the Prescott formula:

$$R_{swl} = Q(0.025 + 0.5n_i)(1 + 0.027z) \quad (\text{A3})$$

where n_i is the daily fractional hours of bright sunshine (dimensionless), which we equate with the one-complement of fractional cloud cover as given in the CRU TS3.1 dataset, and z is elevation (km) above sea level. The second term in brackets is a correction for the thinning of the atmosphere with increasing elevation.

A3 Low-temperature inhibition

Low-temperature inhibition of photosynthesis is accounted for by weighting daily values of PAR (PAR_d) in the accumulation of PAR during a month. We denote the weighted

BGD

11, 3209–3240, 2014

Biophysical constraints on gross primary production

H. Wang et al.

Title Page

Abstract

Introduction

Conclusions

References

Tables

Figures

◀

▶

◀

▶

Back

Close

Full Screen / Esc

Printer-friendly Version

Interactive Discussion



daily and monthly PAR by PAR_{0d} and PAR_0 , respectively. The weighting is calculated as follows:

$$\begin{aligned} PAR_{0d} &= 0 & T_d \leq 0^\circ\text{C} \\ PAR_{0d} &= PAR_d(T_d/10) & 0^\circ\text{C} < T_d < 10^\circ\text{C} \\ PAR_{0d} &= PAR_d & T_d \geq 10^\circ\text{C} \end{aligned} \quad (\text{A4})$$

5 where T_d ($^\circ\text{C}$) is daily temperature, giving

$$PAR_0 = \sum_{i=1}^n PAR_{0d} \quad (\text{A5})$$

where n is the total number of days in the month.

A4 Leaf-internal [CO_2]

The “least-cost” hypothesis states that the sum of the unit costs of maintaining carboxylation and transpiration capacities is minimized. To a good approximation, this applies when the long-term effective value of c_i/c_a is given by $\xi/(\xi + \sqrt{D})$. Here D is an annual effective value of the vapor pressure deficit and ξ is given by $\sqrt{(bK/1.6a)}$ where K is the effective Michaelis–Menten coefficient for Rubisco-limited photosynthesis. The cost factor b is the (assumed conservative) ratio of leaf maintenance respiration to Rubisco carboxylation capacity; the cost factor a is the ratio of sapwood maintenance respiration to transpiration capacity, which is expected to vary with sapwood permeability, plant height (H), and the dynamic viscosity of water (η). We assume that xylem element tapering is perfectly efficient (West et al., 1997, 1999) so the costs of maintaining the transpiration pathway vary only linearly with height (because of the increase in the amount of respiring sapwood) and conductance does not decline due to increasing path length. Efficient tapering is a prerequisite of the pipe model (Shinozaki et al., 1964a, b) that empirically relates sapwood area and subtended leaf area, independently of path length.

Therefore, a can be expressed as a product of H , η and a reference value of a (a_{ref}), and the equation for optimum c_i/c_a can be re-written as:

$$\frac{c_i}{c_a} = \frac{1}{1 + \sqrt{\frac{1.6a_{\text{ref}}H\eta D}{bK}}} \quad (\text{A6})$$

We put the constant terms (1.6, a_{ref} and b) together outside the square root and denote them collectively as C . Equation (A6) can then be simplified to:

$$\frac{c_i}{c_a} = \frac{1}{1 + C\sqrt{\frac{H\eta D}{K}}} \quad (\text{A7})$$

Using a satellite-derived global dataset on vegetation height (Simard et al., 2011), we performed a multiple regression of H against D and *annual* PAR_0 (all three variables log-transformed) yielding the following relationship between H and the other two predictors:

$$H = c \cdot \text{PAR}_0^{0.46} \cdot D^{-0.21} \quad (\text{A8})$$

This relationship is helpful as it suggest a further simplification of Eq. (A7) to allow for the compensating effect of reduced vegetation height in more arid climates. We simply make the approximation $H \propto D^{-0.25}$, leading to:

$$\frac{c_i}{c_a} = \frac{1}{1 + C\sqrt{\frac{\eta}{K}\sqrt{D}}} \quad (\text{A9})$$

Temperature effects are imposed through the known temperature dependencies of η and K (Prentice et al., 2013). The variation of K with elevation takes account of the effect of p_{O} (the partial pressure of oxygen) as $K = K_{\text{C}}(1 + p_{\text{O}}/K_{\text{O}})$ where K_{C} and K_{O} are the Michaelis–Menten coefficients of Rubisco for carboxylation (in the absence of O_2)

Biophysical constraints on gross primary production

H. Wang et al.

Title Page

Abstract

Introduction

Conclusions

References

Tables

Figures

◀

▶

◀

▶

Back

Close

Full Screen / Esc

Printer-friendly Version

Interactive Discussion



and oxygenation, respectively. p_O declines with elevation in proportion to atmospheric pressure (P),

$$P = 101.325e^{-0.114z} \quad (\text{A10})$$

(Jacob, 1999). We estimated C based on the common observation that $c_i/c_a \approx 0.8$ at low elevations in warm, mesic climates. As a reference case we considered $z = 0$ km, $mGDD_0 = 18^\circ\text{C}$ and $\Delta E = 100$ mm (similar to the environment of Sydney, Australia), yielding $C = 14.76$.

Acknowledgements. HW was funded by the Australian Research Council through a Discovery Grant (to ICP and Ian Wright) “Next-generation vegetation model based on functional traits” (grant no. DP120103600), and TWD by Imperial College under a start-up grant to ICP. We thank Brad Evans, Trevor Keenan, Vincent Maire, Ning Dong and Ian Wright for discussions and Brad Evans for helping with the flux partitioning. This paper is a contribution to the AXA Chair Programme on Biosphere and Climate Impacts and Imperial College’s initiative on Grand Challenges in Ecosystems and the Environment. This work used Free Fair-Use eddy covariance data acquired by the FLUXNET community and in particular by the following networks: AmeriFlux (US Department of Energy, Biological and Environmental Research, Terrestrial Carbon Program (DE-FG02-04ER63917 and DE-FG02-04ER63911)), AsiaFlux, CarboEuropeIP, Fluxnet-Canada (supported by CFCAS, NSERC, BIOCAP, Environment Canada, and NRCan), OzFlux, and TCOS-Siberia. We acknowledge the financial support to the eddy covariance data harmonization provided by CarboEuropeIP, FAO-GTOS-TCO, iLEAPS, Max Planck Institute for Biogeochemistry, National Science Foundation, University of Tuscia, Université Laval and Environment Canada and US Department of Energy and the database development and technical support from Berkeley Water Center, Lawrence Berkeley National Laboratory, Microsoft Research eScience, Oak Ridge National Laboratory, University of California–Berkeley, University of Virginia.

BGD

11, 3209–3240, 2014

Biophysical constraints on gross primary production

H. Wang et al.

Title Page

Abstract

Introduction

Conclusions

References

Tables

Figures

⏪

⏩

◀

▶

Back

Close

Full Screen / Esc

Printer-friendly Version

Interactive Discussion



References

- Ahlström, A., Schurgers, G., Arneft, A., and Smith, B.: Robustness and uncertainty in terrestrial ecosystem carbon response to CMIP5 climate change projections, *Environ. Res. Lett.*, 7, 044008, doi:10.1088/1748-9326/7/4/044008, 2012.
- 5 Allen, R. G., Walter, I. A., Elliott, R. L., Howell T. A., Itenfisu, D., Jensen, M. E., and Snyder, R. L.: The ASCE Standardized Reference Evapotranspiration Equation, Amer. Society of Civil Engineers, Reston, Virginia, 2005.
- Anav, A., Friedlingstein, P., Kidston, M., Bopp, L., Ciais, P., Cox, P., Jones, C., Jung, M., Myneni, R., and Zhu, Z.: Evaluating the land and ocean components of the global carbon cycle in the CMIP5 Earth System Models, *J. Climate*, 26, 6801–6843, 2013.
- 10 Arora, V. K., Boer, G. J., Friedlingstein, P., Eby, M., Jones, C. D., Christian, J. R., Bonan, G., Bopp, L., Brovkin, V., and Cadule, P.: Carbon-concentration and carbon-climate feedbacks in CMIP5 Earth System Models, *J. Climate*, 26, 5289–5314, 2013.
- Badawy, B., Rödenbeck, C., Reichstein, M., Carvalhais, N., and Heimann, M.: Technical Note: The Simple Diagnostic Photosynthesis and Respiration Model (SDPRM), *Biogeosciences*, 10, 6485–6508, doi:10.5194/bg-10-6485-2013, 2013.
- 15 Beer, C., Reichstein, M., Tomelleri, E., Ciais, P., Jung, M., Carvalhais, N., Rödenbeck, C., Arain, M. A., Baldocchi, D., and Bonan, G. B.: Terrestrial gross carbon dioxide uptake: global distribution and covariation with climate, *Science*, 329, 834–838, 2010.
- 20 Bernacchi, C. J., Pimentel, C., and Long, S. P.: In vivo temperature response functions of parameters required to model RuBP-limited photosynthesis, *Plant Cell Environ.*, 26, 1419–1430, 2003.
- Bonan, G. B.: Physiological derivation of the observed relationship between net primary production and mean annual air temperature, *Tellus B*, 45, 397–408, 1993.
- 25 Churkina, G. and Running, S. W.: Contrasting climatic controls on the estimated productivity of global terrestrial biomes, *Ecosystems*, 1, 206–215, 1998.
- Ciais, P., Sabine, C., Govindasamy, B., Bopp, L., Brovkin, V., Canadell, J., Chhabra, A., DeFries, R., Galloway, J., Heimann, M., Jones, C., Le Quéré, C., Myneni, R., Piao, S., and Thornton, P.: Carbon and other biogeochemical cycles, in: *Climate Change 2013 The Physical Science Basis*, edited by: Stocker, T., Qin, D., and Plattner, G.-K., Chap. 6, 2013.
- 30

Biophysical constraints on gross primary production

H. Wang et al.

Title Page

Abstract

Introduction

Conclusions

References

Tables

Figures

◀

▶

◀

▶

Back

Close

Full Screen / Esc

Printer-friendly Version

Interactive Discussion



Biophysical constraints on gross primary production

H. Wang et al.

[Title Page](#)

[Abstract](#)

[Introduction](#)

[Conclusions](#)

[References](#)

[Tables](#)

[Figures](#)

[⏪](#)

[⏩](#)

[◀](#)

[▶](#)

[Back](#)

[Close](#)

[Full Screen / Esc](#)

[Printer-friendly Version](#)

[Interactive Discussion](#)



Collatz, G. J., Berry, J. A., and Clark, J. S.: Effects of climate and atmospheric CO₂ partial pressure on the global distribution of C₄ grasses: present, past, and future, *Oecologia*, 114, 441–454, 1998.

Cramer, W. and Prentice, I.: Simulation of regional soil moisture deficits on a European scale, *Norsk Geogr. Tidsskr.*, 42, 149–151, 1988.

Del Grosso, S., Parton, W., Stohlgren, T., Zheng, D., Bachelet, D., Prince, S., Hibbard, K., and Olson, R.: Global potential net primary production predicted from vegetation class, precipitation, and temperature, *Ecology*, 89, 2117–2126, 2008.

DeLUCIA, E., Drake, J. E., Thomas, R. B., and Gonzalez-Meler, M.: Forest carbon use efficiency: is respiration a constant fraction of gross primary production?, *Glob. Change Biol.*, 13, 1157–1167, 2007.

Denman, K. L., Brasseur, G., Chidthaisong, A., Ciacis, P., Cox, P. M., Hauglustaine, D., Heinze, C., Holland, E., Jacob, D., Lohmann, U., Ramachandran, S., Da Silva Dias, P. L., Wofsy, S. C., and Zhang, X.: Couplings between changes in the climate system and biogeochemistry, in: *Climate Change 2007: the Physical Science Basis, Contribution of Working Group I to the Fourth Assessment Report of the Intergovernmental Panel on Climate Change*, edited by: Solomon, S., Qin, D., Manning, M., Chen, Z., Marquis, M., Averyt, K. B., Tignor, M., and Miller, H. L., Cambridge University Press, Cambridge, UK and New York, NY, USA, 2007.

Donohue, R. J., Roderick, M. L., McVicar, T. R., and Farquhar, G. D.: Impact of CO₂ fertilization on maximum foliage cover across the globe's warm, arid environments, *Geophys. Res. Lett.*, 40, 3031–3035, 2013.

Farquhar, G., von Caemmerer, S. V., and Berry, J.: A biochemical model of photosynthetic CO₂ assimilation in leaves of C₃ species, *Planta*, 149, 78–90, 1980.

Fatichi, S., Leuzinger, S., and Körner, C.: Moving beyond photosynthesis: from carbon source to sink-driven vegetation modeling, *New Phytol.*, 201, 1086–1095, doi:10.1111/nph.12614, 2013.

Field, C. B., Randerson, J. T., and Malmström, C. M.: Global net primary production: combining ecology and remote sensing, *Remote Sens. Environ.*, 51, 74–88, 1995.

Friedlingstein, P., Cox, P., Betts, R., Bopp, L., Von Bloh, W., Brovkin, V., Cadule, P., Doney, S., Eby, M., and Fung, I.: Climate-carbon cycle feedback analysis: results from the C4MIP model intercomparison, *J. Climate*, 19, 3337–3353, 2006.

Biophysical constraints on gross primary production

H. Wang et al.

Title Page

Abstract

Introduction

Conclusions

References

Tables

Figures

◀

▶

◀

▶

Back

Close

Full Screen / Esc

Printer-friendly Version

Interactive Discussion



- Friedlingstein, P., Meinshausen, M., Arora, V. K., Jones, C. D., Anav, A., Liddicoat, S. K., and Knutti, R.: Uncertainties in CMIP5 climate projections due to carbon cycle feedbacks, *J. Climate*, 27, 511–526, 2014.
- 5 Friend, A., Woodward, F., and Switsur, V.: Field measurements of photosynthesis, stomatal conductance, leaf nitrogen and $\delta^{13}\text{C}$ along altitudinal gradients in Scotland, *Funct. Ecol.*, 1989, 117–122, 1989.
- Gallego-Sala, A., Clark, J., House, J., Orr, H., Prentice, I. C., Smith, P., Farewell, T., and Chapman, S.: Bioclimatic envelope model of climate change impacts on blanket peatland distribution in Great Britain, *Clim. Res.*, 45, 151–162, 2010.
- 10 Garbulsky, M. F., Peñuelas, J., Papale, D., Ardö, J., Goulden, M. L., Kiely, G., Richardson, A. D., Rotenberg, E., Veenendaal, E. M., and Filella, I.: Patterns and controls of the variability of radiation use efficiency and primary productivity across terrestrial ecosystems, *Global Ecol. Biogeogr.*, 19, 253–267, 2010.
- Gobron, N., Pinty, B., Aussenat, O., Chen, J. M., Cohen, W. B., Fensholt, R., Gond, V., Huemmrich, K. F., Lavergne, T., Melin, F., Privette, J. L., Sandholt, I., Taberner, M., Turner, D. P., Verstraete, M. M., and Widowski, J.-L.: Evaluation of fraction of absorbed photosynthetically active radiation products for different canopy radiation transfer regimes: Methodology and results using Joint Research Center products derived from SeaWiFS against ground-based estimations, *J. Geophys. Res.-Atmos.*, 111, D13110, doi:10.1029/2005JD006511, 2006.
- 20 Haxeltine, A. and Prentice, I. C.: BIOME3: an equilibrium terrestrial biosphere model based on ecophysiological constraints, resource availability, and competition among plant functional types, *Global Biogeochem. Cy.*, 10, 693–709, 1996.
- Hickler, T., Smith, B., Prentice, I. C., Mjöfors, K., Miller, P., Arneth, A., and Sykes, M. T.: CO_2 fertilization in temperate FACE experiments not representative of boreal and tropical forests, *Glob. Change Biol.*, 14, 1531–1542, 2008.
- 25 Hoffman, F. M., Randerson, J. T., Arora, V. K., Bao, Q., Six, K. D., Cadule, P., Ji, D., Jones, C. D., Kawamiya, M., and Khatiwala, S.: Causes and Implications of Persistent Atmospheric Carbon Dioxide Biases in Earth System Models, *J. Geophys. Res.-Biogeo.*, 119, doi:10.1002/2013JG002381, 2014.
- 30 Huston, M. A. and Wolverton, S.: The global distribution of net primary production: resolving the paradox, *Ecol. Monogr.*, 79, 343–377, 2009.
- Jacob, D.: Introduction to atmospheric chemistry, Princeton University Press, 1999.

Biophysical constraints on gross primary production

H. Wang et al.

Title Page

Abstract

Introduction

Conclusions

References

Tables

Figures

◀

▶

◀

▶

Back

Close

Full Screen / Esc

Printer-friendly Version

Interactive Discussion

Jones, C., Robertson, E., Arora, V., Friedlingstein, P., Shevliakova, E., Bopp, L., Brovkin, V., Hajima, T., Kato, E., and Kawamiya, M.: 21st Century compatible CO₂ emissions and airborne fraction simulated by CMIP5 Earth System models under 4 Representative Concentration Pathways, *J. Climate*, 26, 4398–4413, 2013.

5 Kelley, D. I., Prentice, I. C., Harrison, S. P., Wang, H., Simard, M., Fisher, J. B., and Willis, K. O.: A comprehensive benchmarking system for evaluating global vegetation models, *Biogeosciences*, 10, 3313–3340, doi:10.5194/bg-10-3313-2013, 2013.

Kerkhoff, A. J., Enquist, B. J., Elser, J. J., and Fagan, W. F.: Plant allometry, stoichiometry and the temperature-dependence of primary productivity, *Global. Ecol. Biogeogr.*, 14, 585–598, 2005.

10 Knorr, W. and Heimann, M.: Impact of drought stress and other factors on seasonal land biosphere CO₂ exchange studied through an atmospheric tracer transport model, *Tellus B*, 47, 471–489, 1995.

Körner, C. and Diemer, M.: Evidence that plants from high altitudes retain their greater photosynthetic efficiency under elevated CO₂, *Funct. Ecol.*, 8, 58–68, 1994.

15 Kutzbach, J. and Gallimore, R.: Sensitivity of a coupled atmosphere/mixed layer ocean model to changes in orbital forcing at 9000 years BP, *J. Geophys. Res.-Atmos.*, 93, 803–821, 1988.

Linacre, E.: Estimating the net-radiation flux, *Agr. Meteorol.*, 5, 49–63, 1968.

20 Long, S., Postl, W., and Bolhar-Nordenkamp, H.: Quantum yields for uptake of carbon dioxide in C₃ vascular plants of contrasting habitats and taxonomic groupings, *Planta*, 189, 226–234, 1993.

25 Luysaert, S., Inglima, I., Jung, M., Richardson, A. D., Reichstein, M., Papale, D., Piao, S. L., Schulze, E. D., Wingate, L., Matteucci, G., Aragao, L., Aubinet, M., Beer, C., Bernhofer, C., Black, K. G., Bonal, D., Bonnefond, J. M., Chambers, J., Ciais, P., Cook, B., Davis, K. J., Dolman, A. J., Gielen, B., Goulden, M., Grace, J., Granier, A., Grelle, A., Griffis, T., Grünwald, T., Guidolotti, G., Hanson, P. J., Harding, R., Hollinger, D. Y., Hutrya, L. R., Kolar, P., Kruijt, B., Kutsch, W., Lagergren, F., Laurila, T., Law, B. E., Le Maire, G., Lindroth, A., Loustau, D., Malhi, Y., Mateus, J., Migliavacca, M., Misson, L., Montagnani, L., Moncrieff, J., Moors, E., Munger, J. W., Nikinmaa, E., Ollinger, S. V., Pita, G., Rebmann, C., Rouspard, O., Saigusa, N., Sanz, M. J., Seufert, G., Sierra, C., Smith, M. L., Tang, J., Valentini, R., Vesala, T., and Janssens, I. A.: CO₂ balance of boreal, temperate, and tropical forests derived from a global database, *Glob. Change Biol.*, 13, 2509–2537, 2007.

Biophysical constraints on gross primary production

H. Wang et al.

Title Page

Abstract

Introduction

Conclusions

References

Tables

Figures

◀

▶

◀

▶

Back

Close

Full Screen / Esc

Printer-friendly Version

Interactive Discussion



- Maire, V., Martre, P., Kattge, J., Gastal, F., Esser, G., Fontaine, S., and Soussana, J.-F.: The coordination of leaf photosynthesis links C and N fluxes in C3 plant species, *PloS one*, 7, e38345, doi:10.1371/journal.pone.0038345, 2012.
- 5 McCallum, I., Wagner, W., Schmulilius, C., Shvidenko, A., Obersteiner, M., Fritz, S., and Nilsson, S.: Comparison of four global FAPAR datasets over Northern Eurasia for the year 2000, *Remote Sens. Environ.*, 114, 941–949, 2010.
- Mercado, L. M., Bellouin, N., Sitch, S., Boucher, O., Huntingford, C., Wild, M., and Cox, P. M.: Impact of changes in diffuse radiation on the global land carbon sink, *Nature*, 458, 1014–1017, 2009.
- 10 Monteith, J. and Moss, C.: Climate and the efficiency of crop production in Britain [and discussion], *Philos. T. Roy. Soc. B*, 281, 277–294, 1977a.
- Monteith, J. L. and Moss, C. J.: Climate and the efficiency of crop production in Britain [and Discussion], *Philos. T. Roy. Soc. B*, 281, 277–294, 1977b.
- Norby, R. J., DeLucia, E. H., Gielen, B., Calfapietra, C., Giardina, C. P., King, J. S., Ledford, J., McCarthy, H. R., Moore, D. J., and Ceulemans, R.: Forest response to elevated CO₂ is conserved across a broad range of productivity, *P. Natl. Acad. Sci. USA*, 102, 18052–18056, 2005.
- 15 Pickett-Heaps, C. A., Canadell, J. G., Briggs, P. R., Gobron, N., Haverd, V., Paget, M. J., Pinty, B., and Raupach, M. R.: Evaluation of six satellite-derived Fraction of Absorbed Photosynthetic Active Radiation (FAPAR) products across the Australian continent, *Remote Sens. Environ.*, 140, 241–256, 2014.
- Pongratz, J., Lobell, D., Cao, L., and Caldeira, K.: Crop yields in a geoeingeneered climate, *Nature Climate Change*, 2, 101–105, 2012.
- Poorter, H., Niklas, K. J., Reich, P. B., Oleksyn, J., Poot, P., and Mommer, L.: Biomass allocation to leaves, stems and roots: meta-analyses of interspecific variation and environmental control, *New Phytol.*, 193, 30–50, 2012.
- 20 Potter, C. S., Randerson, J. T., Field, C. B., Matson, P. A., Vitousek, P. M., Mooney, H. A., and Klooster, S. A.: Terrestrial ecosystem production: a process model based on global satellite and surface data, *Global Biogeochem. Cy.*, 7, 811–841, 1993.
- 30 Prentice, I. C., Dong, N., Gleason, S. M., Maire, V., and Wright, I. J.: Balancing the costs of carbon gain and water transport: testing a new theoretical framework for plant functional ecology, *Ecol. Lett.*, 17, 82–91, 2013.

Biophysical constraints on gross primary production

H. Wang et al.

Title Page

Abstract

Introduction

Conclusions

References

Tables

Figures

◀

▶

◀

▶

Back

Close

Full Screen / Esc

Printer-friendly Version

Interactive Discussion



- Ruimy, A., Jarvis, P. G., Baldocchi, D. D., and Saugier, B.: CO₂ fluxes over plant canopies and solar radiation: a review, *Adv. Ecol. Res.*, 26, 1–68, 1995.
- Running, S. W., Nemani, R. R., Heinsch, F. A., Zhao, M., Reeves, M., and Hashimoto, H.: A continuous satellite-derived measure of global terrestrial primary production, *Bioscience*, 54, 547–560, 2004.
- Shinozaki, K., Yoda, K., Hozumi, K., and Kira, T.: A quantitative analysis of plant form-the pipe model theory: I. Basic analyses, *Jpn. J. Ecol.*, 14, 97–105, 1964a.
- Shinozaki, K., Yoda, K., Hozumi, K., and Kira, T.: A quantitative analysis of plant form-the pipe model theory: II. Further evidence of the theory and its application in forest ecology, *Jpn. J. Ecol.*, 14, 133–139, 1964b.
- Simard, M., Pinto, N., Fisher, J. B., and Baccini, A.: Mapping forest canopy height globally with spaceborne lidar, *J. Geophys. Res.*, 116, G04021, doi:10.1029/2011JG001708, 2011.
- Sitch, S., Smith, B., Prentice, I. C., Arneth, A., Bondeau, A., Cramer, W., Kaplan, J. O., Levis, S., Lucht, W., Sykes, M. T., Thonicke, K., and Venevsky, S.: Evaluation of ecosystem dynamics, plant geography and terrestrial carbon cycling in the LPJ dynamic global vegetation model, *Glob. Change Biol.*, 9, 161–185, 2003.
- Sitch, S., Huntingford, C., Gedney, N., Levy, P., Lomas, M., Piao, S., Betts, R., Ciais, P., Cox, P., and Friedlingstein, P.: Evaluation of the terrestrial carbon cycle, future plant geography and climate-carbon cycle feedbacks using five Dynamic Global Vegetation Models (DGVMs), *Glob. Change Biol.*, 14, 2015–2039, 2008.
- Sykes, M. T., Prentice, I. C., and Cramer, W.: A bioclimatic model for the potential distributions of north European tree species under present and future climates, *J. Biogeogr.*, 23, 203–233, 1996.
- Thomas, R. Q., Zaehle, S., Templer, P. H., and Goodale, C. L.: Global patterns of nitrogen limitation: confronting two global biogeochemical models with observations, *Glob. Change Biol.*, 19, 2986–2998, 2013.
- Todd-Brown, K. E. O., Randerson, J. T., Post, W. M., Hoffman, F. M., Tarnocai, C., Schuur, E. A. G., and Allison, S. D.: Causes of variation in soil carbon simulations from CMIP5 Earth system models and comparison with observations, *Biogeosciences*, 10, 1717–1736, doi:10.5194/bg-10-1717-2013, 2013.
- Ukkola, A. M. and Prentice, I. C.: A worldwide analysis of trends in water-balance evapotranspiration, *Hydrol. Earth Syst. Sci. Discuss.*, 10, 5739–5765, doi:10.5194/hessd-10-5739-2013, 2013.

Biophysical constraints on gross primary production

H. Wang et al.

Title Page

Abstract

Introduction

Conclusions

References

Tables

Figures

◀

▶

◀

▶

Back

Close

Full Screen / Esc

Printer-friendly Version

Interactive Discussion



Wang, H., Prentice, I. C., and Ni, J.: Primary production in forests and grasslands of China: contrasting environmental responses of light- and water-use efficiency models, *Biogeosciences*, 9, 4689–4705, doi:10.5194/bg-9-4689-2012, 2012.

Waring, R., Landsberg, J., and Williams, M.: Net primary production of forests: a constant fraction of gross primary production?, *Tree Physiol.*, 18, 129–134, 1998.

Weedon, G. P., Gomes, S., Balsamo, G., Best, M. J., Bellouin, N., and Viterbo, P.: WATCH forcing databased on ERA-INTERIM, available at: ftp://rfddata:forceDATA@ftp.iiasa.ac.at (last access: 24 July 2012), 2012.

Welp, L. R., Keeling, R. F., Meijer, H. A., Bollenbacher, A. F., Piper, S. C., Yoshimura, K., Francey, R. J., Allison, C. E., and Wahlen, M.: Interannual variability in the oxygen isotopes of atmospheric CO₂ driven by El Niño, *Nature*, 477, 579–582, 2011.

West, G. B., Brown, J. H., and Enquist, B. J.: A general model for the origin of allometric scaling laws in biology, *Science*, 276, 122–126, 1997.

West, G. B., Brown, J. H., and Enquist, B. J.: A general model for the structure and allometry of plant vascular systems, *Nature*, 400, 664–667, 1999.

Willson, R. C. and Mordvinov, A. V.: Secular total solar irradiance trend during solar cycles 21–23, *Geophys. Res. Lett.*, 30, 1199, 2003.

Wright, I. J., Reich, P. B., and Westoby, M.: Least-cost input mixtures of water and nitrogen for photosynthesis, *Am. Nat.*, 161, 98–111, 2003.

Zaehle, S. and Dalmonch, D.: Carbon–nitrogen interactions on land at global scales: current understanding in modelling climate biosphere feedbacks, *Current Opinion in Environmental Sustainability*, 3, 311–320, 2011.

Biophysical constraints on gross primary production

H. Wang et al.

Table 1. Model equations for each step and the global annual GPP (PgCa^{-1}) estimated by each model.

Model equation	Global GPP
$\text{GPP} = \varphi_0 \cdot a \cdot \text{PAR}_{\text{toa}}$	2960
$\text{GPP} = \varphi_0 \cdot a \cdot \text{PAR}$	1442
$\text{GPP} = \varphi_0 \cdot a \cdot \text{PAR} \cdot \text{fAPAR}$	322
$\text{GPP} = \varphi_0 \cdot a \cdot \text{PAR}_0 \cdot \text{fAPAR}$	300
$\text{GPP} = \varphi_0 \cdot a \cdot \text{PAR}_0 \cdot \text{fAPAR} \cdot \frac{c_i - \Gamma^*}{c_i + 2\Gamma^*}$	210

Title Page

Abstract

Introduction

Conclusions

References

Tables

Figures

⏪

⏩

◀

▶

Back

Close

Full Screen / Esc

Printer-friendly Version

Interactive Discussion



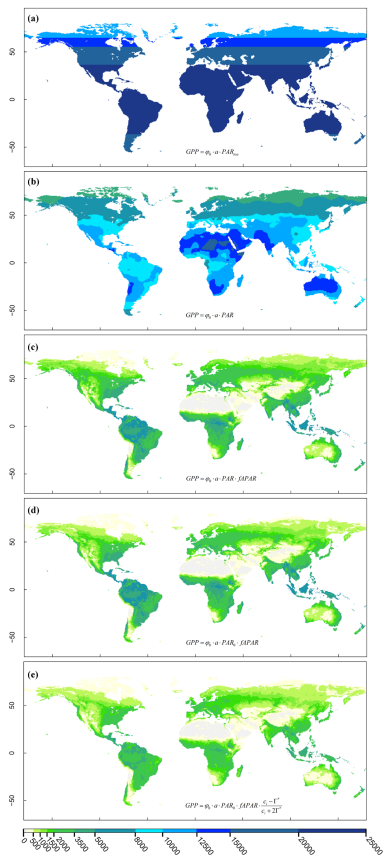


Fig. 1. The patterns of modelled global annual GPP ($\text{gC m}^{-2} \text{a}^{-1}$) controlled by PAR at the top of atmosphere **(a)**, and modified by a sequence of effects: atmospheric transmissivity and cloud cover **(b)**, foliage cover **(c)**, low-temperature inhibition **(d)** and CO_2 limitation **(e)**.

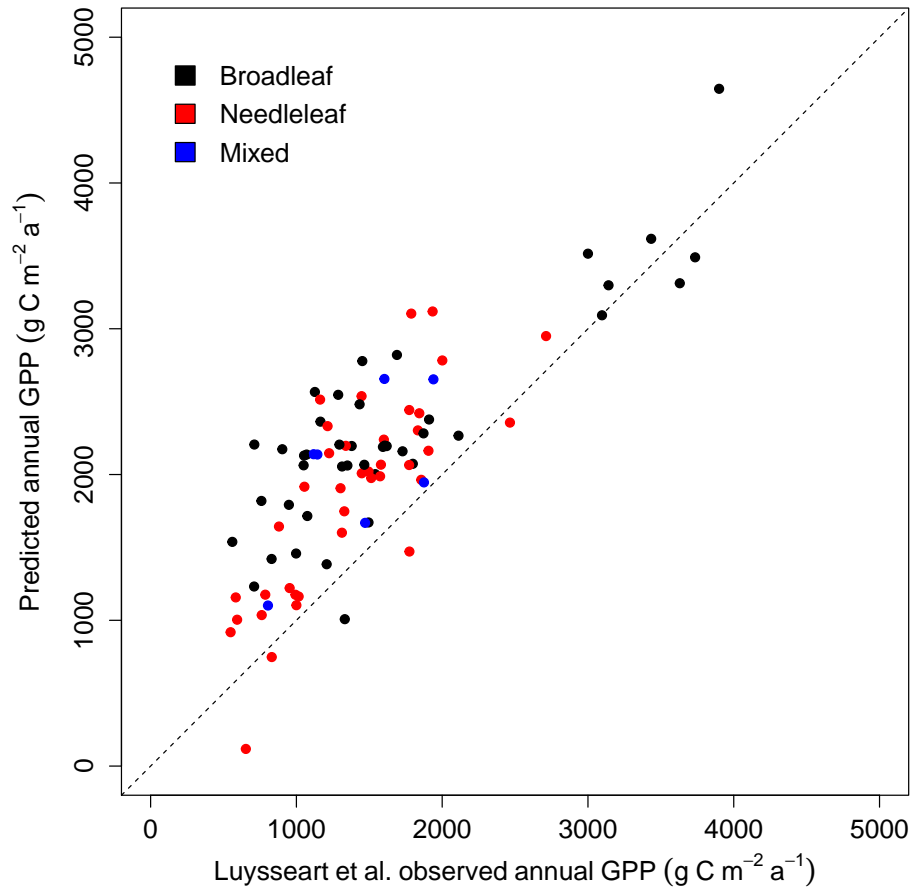


Fig. 2. Relationship between observed annual GPP from Luysaert et al. (2007) and predicted annual GPP.

BGD

11, 3209–3240, 2014

Biophysical constraints on gross primary production

H. Wang et al.

Title Page

Abstract

Introduction

Conclusions

References

Tables

Figures

◀

▶

◀

▶

Back

Close

Full Screen / Esc

Printer-friendly Version

Interactive Discussion



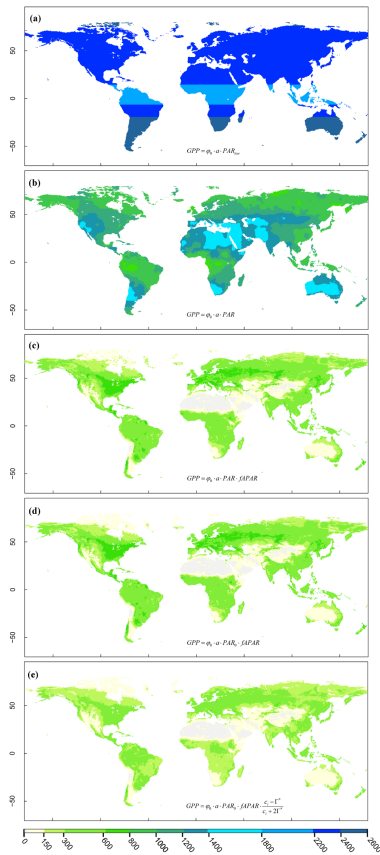


Fig. 3. The patterns of modelled global maximum monthly GPP ($\text{gCm}^{-2}\text{month}^{-1}$) controlled by PAR at the top of atmosphere (a), and modified by a sequence of effects as in Fig. 1.

Biophysical constraints on gross primary production

H. Wang et al.

Title Page

Abstract Introduction

Conclusions References

Tables Figures

◀ ▶

◀ ▶

Back Close

Full Screen / Esc

Printer-friendly Version

Interactive Discussion



Biophysical constraints on gross primary production

H. Wang et al.

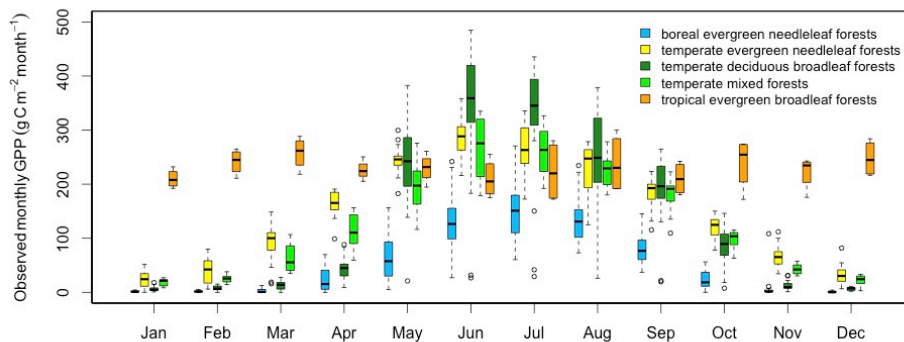


Fig. 4. Box-and-whisker plot of monthly GPP ($\text{g C m}^{-2} \text{ month}^{-1}$) vs. month, based on gap-filled GPP observations derived from the publicly available measurements in the FLUXNET archive. The bottom of the box is the lower quartile and the top is the upper quartile. The whiskers extend to the lower and upper extremes, beyond which outliers are defined and plotted as dots.

Title Page

Abstract

Introduction

Conclusions

References

Tables

Figures

◀

▶

◀

▶

Back

Close

Full Screen / Esc

Printer-friendly Version

Interactive Discussion

